Supporting Information

Theoretical Prediction and Experimentally Realizing Cathodic Doping of Sulfur in $Li_4Ti_5O_{12}$ for Superior Lithium Storage Performance

Mengyao Shen[a], Jianfeng Zhu[a], Shangqi Sun, Daming Chen, Fei Liu, Jian Chen*

Jiangsu Key Laboratory of Advanced Metallic Materials, School of Materials Science and Engineering, Southeast University, Nanjing 211189, China

* Corresponding author

E-mail: j.chen@seu.edu.cn (J.C.).

[a] These authors contribute equally to this work

1. Structural analysis

In $Li_{32}Ti_{40}O_{96}$, the fractional coordinates of 16d Li are as follows

(0.375, 0.875, 0.125), (0.625, 0.625, 0.625), (0.125, 0.375, 0.875), (0.875, 0.125, 0.458), (0.375, 0.375, 0.542), (0.625, 0.125, 0.708), (0.125, 0.875, 0.792), (0.875, 0.625, 0.958)

2. Defect formation energy

The chemical potential of $Li_4Ti_5O_{12}$ ($\mu_{Li_4Ti_5O_{12}}$), which represents the energy of each chemical molecular unit in a perfect $Li_4Ti_5O_{12}$ crystal, can be described by

$$\mu_{Li_4Ti_5O_{12}(bulk)} = 4\mu_{Li} + 5\mu_{Ti} + 12\mu_{O}.$$

The three adjacent phases in equilibrium were used to to determine the chemical potentials of μ_{Ti}, μ_O and μ_{Li} at points A-G. For instance, at point A, the $Li_4Ti_5O_{12}$, Li_2O and Li_2O_2 phases are in equilibrium. Therefore, the μ_i of the element follows

the following equation.

$$\mu_O = \mu_{Li_2O_2(bulk)} - \mu_{Li_2O(bulk)}$$

$$\mu_{Li} = \frac{1}{2}[2\mu_{Li_2O(bulk)} - \mu_{Li_2O_2(bulk)}]$$

$$\mu_{Ti} = \frac{1}{5}[\mu_{Li_4Ti_5O_{12}(bulk)} - 12\mu_O - 4\mu_{Li}]$$

Where μ_O, μ_{Li}, $\mu_{Li_2O_2(bulk)}$ and $\mu_{Li_2O(bulk)}$ are the chemical potentials of O_2, Li, Li_2O_2 and Li_2O. Similar calculation steps for point B-G are given as below.

Phase point B：

$$\mu_O = \frac{1}{2}\mu_{O_2(bulk)}$$

$$\mu_{Li} = \frac{1}{2}[\mu_{Li_2O_2(bulk)} - \mu_{O_{2(bulk)}}]$$

$$\mu_{Ti} = \frac{1}{5}[\mu_{Li_4Ti_5O_{12}(bulk)} - 4\mu_{Li} - 12\mu_O]$$

Phase point C：

$$\mu_O = \frac{1}{2}\mu_{O_2(bulk)}$$

$$\mu_{Ti} = \mu_{TiO_2(bulk)} - \mu_{O_2(bulk)}$$

$$\mu_{Li} = \frac{1}{4}[\mu_{Li_4Ti_5O_{12}(bulk)} - 12\mu_O - 5\mu_{Ti}]$$

Phase point D：

$$\mu_O = 2\mu_{TiO_2(bulk)} - \mu_{Ti_2O_3(bulk)}$$

$$\mu_{Ti} = 2\mu_{Ti_2O_3(bulk)} - 3\mu_{TiO_2(bulk)}$$

$$\mu_{Li} = \frac{1}{4}[\mu_{Li_4Ti_5O_{12}(bulk)} - 12\mu_O - 5\mu_{Ti}]$$

Phase point E：

$$\mu_O = \frac{1}{3}[\mu_{Ti_2O_3(bulk)} - 2\mu_{Ti}]$$

$$\mu_{Ti} = \mu_{Ti(bulk)}$$

$$\mu_{Li} = \frac{1}{4}[\mu_{Li_4Ti_5O_{12}(bulk)} - 12\mu_O - 5\mu_{Ti}]$$

Phase point F:

$$\mu_O = \frac{1}{12}[\mu_{Li_4Ti_5O_{12}(bulk)} - 4\mu_{Li} - 5\mu_{Ti}]$$

$$\mu_{Ti} = \mu_{Ti(bulk)}$$

$$\mu_{Li} = \mu_{Li(bulk)}$$

Phase point G:

$$\mu_O = \mu_{Li_2O(bulk)} - 2\mu_{Li}$$

$$\mu_{Ti} = \frac{1}{5}[\mu_{Li_4Ti_5O_{12}(bulk)} - 4\mu_{Li} - 12\mu_O]$$

$$\mu_{Li} = \mu_{Li(bulk)}$$

Table S1. Total energies of pure $(Li_4Ti_5O_{12})_8$ and S-doped $(Li_4Ti_5O_{12})_8$ supercells

Compound	Total energy (eV)
$Li_{32}Ti_{40}O_{96}$	-1333.363
$Li_{32}Ti_{39}SO_{96}$	-1317.600
$Li_{32}Ti_{40}O_{95}S$	-1320.311

Table S2. The chemical potentials of related compounds

Compound	Chemical potential (eV)
S	-7.316
SO_2	-17.208
O_2	-9.892
Ti	-7.833
Li	-1.750
Li_2O	-14.314
Li_2O_2	-19.403
TiO_2	-26.934
Ti_2O_3	-44.912
$Li_4Ti_5O_{12}$	-165.625

Table S3. Calculated formation energies of relevant compounds at 0 K per formula unit along with reported results

Compound	Space group	Formation Energy (eV)		
		This work	Calculated results [1]	Experimental results [2-3]
Ti_2O_3	*R-3c*	-14.41	-14.28	-16.60
TiO_2	*$I4_1/amd$*	-9.99	-9.12	-10.56
Li_2O	*Fm-3m*	-5.86	-5.60	-6.22
Li_2O_2	*$P6_3/mmc$*	-6.01	-5.71	-6.58
$Li_4Ti_5O_{12}$	*Fd-3m*	-20.21	-19.35	-

Table S4. Defect formation energy at point A-G

Point	Ti-S(eV)	O-S(eV)
A	5.657	15.279
B	2.575	15.422
C	6.037	15.422
D	14.057	11.412
E	15.246	10.619
F	15.246	10.303
G	17.107	9.556

Table S5. Discharge capacity of the S-doped $Li_4Ti_5O_{12}$ electrode prepared in this work as well as of those of analogous doped $Li_4Ti_5O_{12}$ materials reported in previous studies

Doping element	Electrode Material	Discharge Capacity (mAh g^{-1})	Rate(C)	Reference
S	S doped $Li_4Ti_5O_{12}$	176.0 (250 cycles) 147.6 (1000 cycles) 126.4 (1000 cycles)	1C 5C 20C	This work
P	P doped $Li_4Ti_5O_{12}$	156.0 (160 cycles)	1C	[4]
Zn	$Li_4Zn_{0.05}Ti_5O_{12}$	141.7 (1000 cycles)	5C	[5]
Ca	$Li_{3.9}Ca_{0.1}Ti_5O_{12}$	162.4 (100 cycles) 148.8 (100 cycles) 138.7 (100 cycles)	1C 5C 10C	[6]
V	$Li_4Ti_{4.9}V_{0.1}O_{12}$	136.4 (1713 cycles) 103.0 (400 cycles)	2C 5C	[7]
Cr	$Li_{4-x}Cr_{3x}Ti_{5-2x}O_{12}$ (x = 0.1)	155.0 (1000 cycles)	1C	[8]
W	$Li_4Ti_{4.9}W_{0.1}O_{12}$	128.1 (100 cycles)	10C	[9]
Nb	$Li_4Ti_{4.95}Nb_{0.05}O_{12}$	169.1 (100 cycles) 115.7 (100 cycles)	1C 10C	[10]
Ta	$Li_4Ti_{4.995}Ta_{0.005}O_{12}$	132.2 (50 cycles)	5C	[11]
Na	$Li_{4-x}Na_xTi_5O_{12}$	$Li_{4-x}Na_xTi_5O_{12}$(x=0.1) 133.0 (200 cycles) $Li_{4-x}Na_xTi_5O_{12}$(x=0.15) 135.0 (200 cycles)	5C	[12]
K	$Li_{3.98}Na_{0.01}K_{0.01}Ti_5O_{12}$	165.0 (50 cycles)	1C	[13]
Al	$Li_4Ti_{4.85}Al_{0.15}O_{12}$ $Li_{3.85}Al_{0.15}Ti_5O_{12}$	$Li_4Ti_{4.85}Al_{0.15}O_{12}$: 101.0(100 cycles) $Li_{3.85}Al_{0.15}Ti_5O_{12}$: 88.0 (100 cycles)	1C	[14]
Br	$Li_4Ti_5O_{12-x}Br_x$ (x=0.2)	159.0 (50 cycles) 150.2 (50 cycles)	0.5C 1C	[15]

Table S6. The initial specific capacities

Sample	5C			20C		
	Initial specific capacitiy (mA h g^{-1})	Specific capacity after 1000 cylces (mA h g^{-1})	Capacity retention rate	Initial specific capacitiy (mA h g^{-1})	Specific capacity after 1000 cylces (mA h g^{-1})	Capacity retention rate
LTO	122.1	95.7	78.4%	139.8	98.2	70.2%
SLTO	170.4	147.6	86.6%	160.4	126.4	78.8%

Table S7. Atomic charges (in e) for Li, Ti, O and S as obtained from a purely ionic model (Qi), Bader analysis (Q^B) and their differences ($Q = Q^B - Q^i$).

Compounds	Atoms	Bader electrons(Q^B)	Q^i	$Q= Q^B- Q^i$
$Li_{32}Ti_{40}O_{96}$	Li (8a)	2.11	3	-0.89
	Li (16d)	2.12	3	-0.88
	Ti (16d)	7.89	10	-2.11
	O (32e)	7.17	6	+1.17
$Li_{32}Ti_{39}SO_{96}$	Li (8a)	2.11	3	-0.89
	Li (16d)	2.12	3	-0.88
	Ti (16d)	7.89	10	-2.11
	O (32e)	7.17	6	+1.17
	S(16d)	4.23	6	-1.77

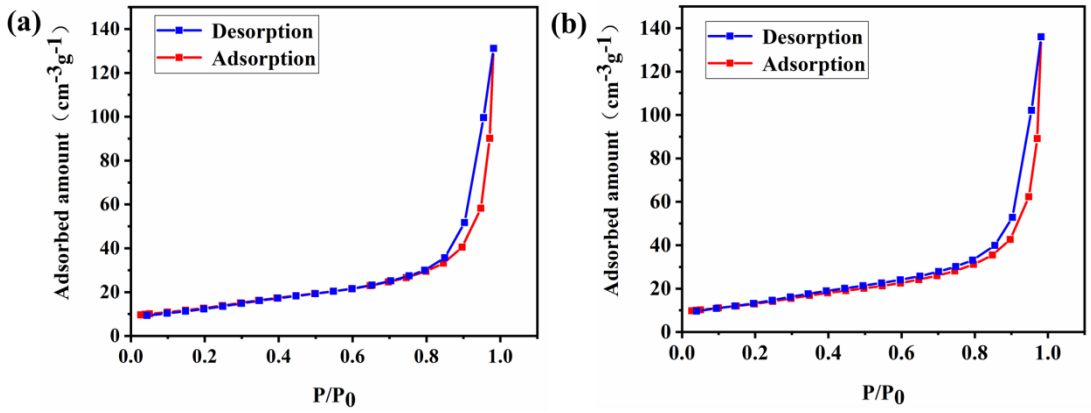

Figure S1. Nitrogen adsorption-desorption isotherm of (a)LTO (b)SLTO.

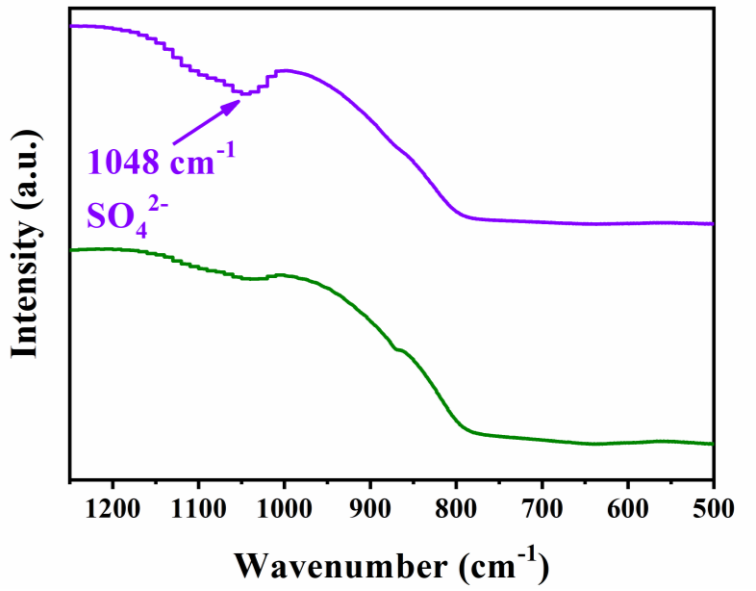

Figure S2. FTIR spectra of LTO and SLTO

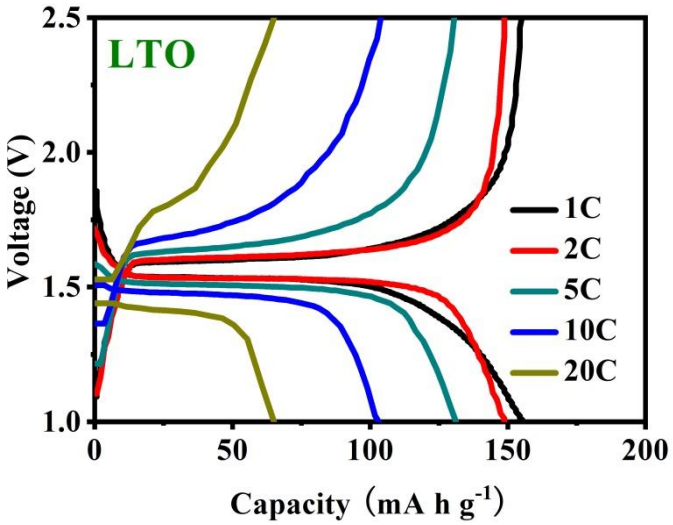

Figure S3. Discharge/charge curves of LTO

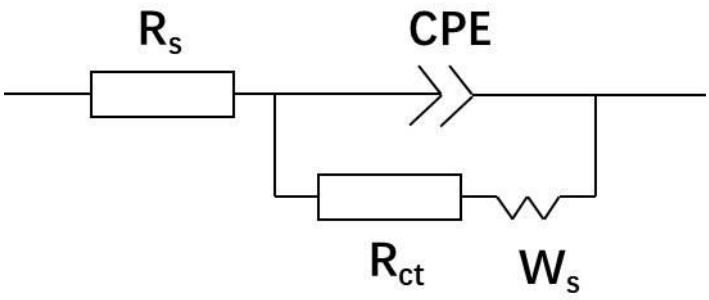

Figure S4. EIS equivalent circuit diagram

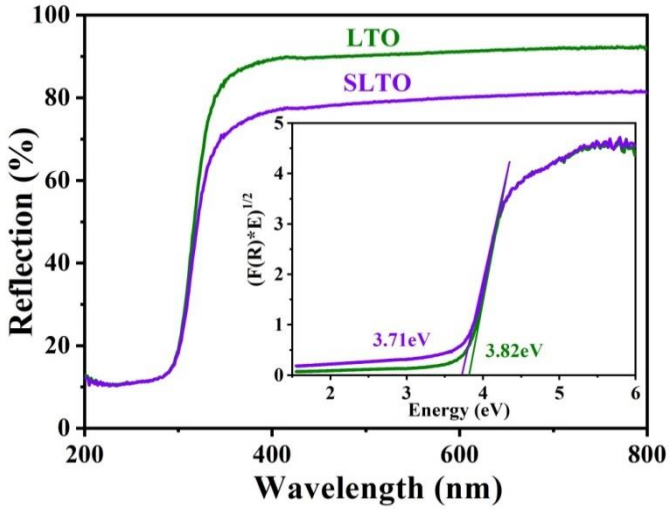

Figure S5. UV-vis DRS spectra of LTO and SLTO

References:

[1] Duan, H.; Li, J.; Du, H.; Chiang, S. W.; Xu, C.; Duan, W.; Kang, F. Tailoring Native Defects and Zinc Impurities in $Li_4Ti_5O_{12}$: Insights from First-Principles Study. *The Journal of Physical Chemistry C* **2015**, *119*, 5238-5245.

[2] Jain, A.; Ong, S. P.; Hautier, G.; Chen, W.; Richards, W. D.; Dacek, S.; Cholia, S.; Gunter, D.; Skinner, D.; Ceder, G.et al. Commentary: The Materials Project: A materials genome approach to accelerating materials innovation. *APL Materials* **2013**, *1*, 11002.

[3] Ong, S. P.; Richards, W. D.; Jain, A.; Hautier, G.; Kocher, M.; Cholia, S.; Gunter, D.; Chevrier, V. L.; Persson, K. A.; Ceder, G. Python Materials Genomics (pymatgen): A robust, open-source python library for materials analysis. *Comp. Mater. Sci.* **2013**, *68*, 314-319.

[4] Deng, W.; Feng, X.; Li, X.; O'Neill, S.; Hu, L.; Liu, L.; Wong, W.; Hu, Y.; Li, C. M. Improving the electrochemical performance of $Li_4Ti_5O_{12}$ anode by phosphorus reduction at a relatively low temperature. *Chem. Commun.* **2018**, *54*, 14120-14123.

[5] Xueyang Ji, Q. L. E. G. Bamboo-Shaped Zn^{2+}-Doped $Li_4Ti_5O_{12}$ Nanofibers: One-Step Controllable Synthesis and High-Performance Lithium-Ion Batteries. *J. Electrochem. Soc.* **2018**.

[6] Zhang, Q.; Zhang, C.; Li, B.; Kang, S.; Li, X.; Wang, Y. Preparation and electrochemical properties of Ca-doped Li4Ti5O12 as anode materials in lithium-ion battery. *Electrochim. Acta* **2013**, *98*, 146-152.

[7] Yu, Z.; Zhang, X.; Yang, G.; Liu, J.; Wang, J.; Wang, R.; Zhang, J. High rate capability and long-term cyclability of $Li_4Ti_{4.9}V_{0.1}O_{12}$ as anode material in lithium ion battery. *Electrochim. Acta* **2011**, *56*, 8611-8617.

[8] Zou, H.; Liang, X.; Feng, X.; Xiang, H. Chromium-Modified $Li_4Ti_5O_{12}$ with a Synergistic Effect of Bulk Doping, Surface Coating, and Size Reducing. *ACS Appl. Mater. Inter.* **2016**, *8*, 21407-21416.

[9] Zhang, Q.; Zhang, C.; Li, B.; Jiang, D.; Kang, S.; Li, X.; Wang, Y. Preparation and characterization of W-doped $Li_4Ti_5O_{12}$ anode material for enhancing the high rate performance. *Electrochim. Acta* **2013**, *107*, 139-146.

[10] Tian, B.; Xiang, H.; Zhang, L.; Li, Z.; Wang, H. Niobium doped lithium titanate as a high rate anode material for Li-ion batteries. *Electrochim. Acta* **2010**, *55*, 5453-5458.

[11] Guo, M.; Wang, S.; Ding, L.; Huang, C.; Wang, H. Tantalum-doped lithium titanate with enhanced performance for lithium-ion batteries. *J. Power Sources* **2015**, *283*, 372-380.

[12] Yi, T.; Yang, S.; Li, X.; Yao, J.; Zhu, Y.; Zhu, R. Sub-micrometric $Li_{4-x}Na_xTi_5O_{12}$ ($0 \leqslant x \leqslant 0.2$) spinel as anode material exhibiting high rate capability. *J. Power Sources* **2014**, *246*, 505-511.

[13] Liu, Z.; Sun, L.; Yang, W.; Yang, J.; Han, S.; Chen, D.; Liu, Y.; Liu, X. The synergic effects of Na and K co-doping on the crystal structure and electrochemical properties of $Li_4Ti_5O_{12}$ as anode material for lithium ion battery. *Solid State Sci.* **2015**, *44*, 39-44.

[14] Ncube, N. M.; Mhlongo, W. T.; McCrindle, R. I.; Zheng, H. The electrochemical effect of Al-doping on $Li_4Ti_5O_{12}$ as anode material for lithium-ion batteries. *Materials today : proceedings* **2018**, *5*, 10592-10601.

[15] Qi, Y.; Huang, Y.; Jia, D.; Bao, S.; Guo, Z. P. Preparation and characterization of novel spinel $Li_4Ti_5O_{12-x}Br_x$ anode materials. *Electrochim. Acta* **2009**, *54*, 4772-4776.